



Co-published by
Institute of Fluid-Flow Machinery
Polish Academy of Sciences
Committee on Thermodynamics and Combustion
Polish Academy of Sciences

Copyright©2025 by the Authors under licence CC BY-NC-ND 4.0

<http://www.imp.gda.pl/archives-of-thermodynamics/>



Numerical study of radiative MHD hybrid nanofluid flow through porous concentric cylinders

Rudrappa Mahesha^{a,b}, Narasappa Nalinakshi^a, Thavada Sravan Kumar^{a*}

^aDepartment of Mathematics, Atria Institute of Technology, Bengaluru 560024, KA, India.

^bVisvesvaraya Technological University, Belagavi 590018, KA, India.

*Corresponding author email: sravan.k@atria.edu

Received: 28.10.2024; revised: 31.12.2024; accepted: 31.12.2024

Abstract

The main objective of this study is to investigate the effects of Cu, Al₂O₃, and H₂O-based nanofluids on heat transfer through annulus-shaped, two concentric cylindrical regions. The quadratic convection in the flow of hybrid nanofluids in an inclined porous annulus medium is considered. The conservation laws are obeyed in a non-linear model of the flow geometry. Applying a suitable non-dimensional transformation, we solved the resultant equation using the Runge-Kutta 4th order method with a shooting technique to obtain the solution for the velocity and temperature. The flow structure and heat transfer are influenced by quadratic resistance and mixed convection mechanisms in nonlinear Boussinesq approximation, as investigated in biomedical devices, nuclear reactors as well as heat exchangers. The analysis demonstrates that radiation significantly affects heat transfer by enhancing the Lorentz force, which in turn dissipates the flow rate. This behaviour aligns well with the flow patterns reported in previous studies for various physical parameters.

Keywords: Magnetohydrodynamics; Irregular heat source; Hybrid nanofluids; Heat transfer; Concentric cylinder

Vol. 46(2024), No. 1, 201–208; doi: 10.24425/ather.2025.154194

Cite this manuscript as: Mahesha, R., Nalinakshi, N., & Sravan Kumar, T. (2025). Numerical Study of Radiative MHD Hybrid Nanofluid Flow through Porous Concentric Cylinders. *Archives of Thermodynamics*, 46(1), 201–208.

1. Introduction

Many researchers have recently diverted their interest to nanotechnology innovation as it offers a variety of opportunities for designing and manufacturing goods with advancements in heat transfer. Hybrid nanofluids flowing across an annular cylindrical region are used in nuclear power plants, hot rollers, heat exchangers and heat storage systems to transfer heat. The nanofluid has colloidal suspensions of nanoparticles in a base fluid. Choi and Eastman [1] reported on investigating nanofluids and heat characteristics.

The term ‘hybrid’ describes the combination of various unique nanoparticles that create a homogeneous phase. The metal

and metal oxide nanoparticles such as Al, Cu, Fe, MgO, Al₂O₃, TiO₂ and SiO₂ are disseminated in oil, water, kerosene and ethylene glycol (base fluids). The wide range of applications of hybrid nanofluids has a revolutionary approach to heat transfer accepted among researchers. A conventional fluid that contains both metallic and non-metallic nanoparticles has enhanced thermophysical properties, which demonstrated that the hybrid nanofluids (Al₂O₃-Cu-H₂O) had a higher diffusivity than the mononanofluids described by Suresh et al. [2]. Devi and Devi [3] and Kanchana et al. [4] investigated stiff isothermal boundary conditions in heat transfer and show an improvement in the fraction factor for the suspension of two nanoparticles in water. Waini et al. [5] found that Cu-Al₂O₃ has a higher heat transfer

Nomenclature

- a – radius of the inner cylinder, m
 b – radius of the outer cylinder, m
 B_0 – magnetic field, T
 Bi_1 – Biot number cylinder 1, $Bi_1 = \frac{h_1 a}{\kappa_f}$
 Bi_2 – Biot number cylinder 2, $Bi_2 = \frac{h_2 a}{\kappa_f}$
 C_p – specific heat at constant pressure, kJ/(kg K)
 Da – Darcy number
 Ec – Eckert number, $Ec = \frac{U_w^2}{(c_p)_f(T_w - T_\infty)}$
 g – gravitational acceleration, m/s²
 h_1, h_2 – convective heat transport coefficients, W/(m²·K)
 M – magnetic parameter, $M = \sqrt{\frac{\sigma \beta_0^2 a^2}{\mu_f}}$
 Mc – mixed convection parameter, $Mc = \frac{g(\rho\beta_0)_f(T_w - T_0)a^2}{u_0 \mu_f}$
 m – shape factor of different nanoparticles
 N – radiation parameter, $N = \frac{4\sigma T_0^3}{\chi \kappa_f}$
 Nu – Nusselt number
 n – exponential index
 Pr – Prandtl number, $Pr = \frac{(\mu c_p)_f}{\kappa_f}$
 p – pressure, kPa
 Q_0 – THS coefficient
 Q_e – ESHS coefficient
 Q_C – quadratic convection parameter, $Q_C = \frac{(\rho\beta_1)_f(T_w - T_0)}{(\rho\beta_0)_f}$
 Q_E – exponential space-related heat source parameter, $Q_E = \frac{Q_e a^2}{v_f(\rho c_p)_f}$
 Q_T – temperature related heat source parameter, $Q_T = \frac{Q_0 a^2}{v_f(\rho c_p)_f}$

- R – dimensionless radial axis
 r – radial axis
 T – temperature, K
 U – nondimensional velocity, m/s
 u – dimensional velocity, m/s
 z – common axis

Greek symbols

- α – angle of inclination, rad
 β – thermal expansion coefficient, K⁻¹
 θ – nondimensional temperature, K
 κ – thermal conductivity, W/(m·K)
 λ – aspect ratio,
 μ – dynamic viscosity, Pa·s
 ν – kinematic viscosity, m²/s
 σ – Stefan Boltzmann constant, W/(m² K⁴)
 ρ – density, kg/m³
 τ – skin friction coefficient
 ϕ – volume fraction

Subscripts and Superscripts

- hnf – hybrid nanofluids
 nf – nanofluids
 f – fluids

Abbreviations and Acronyms

- LBA – linear Boussinesq approximation
 NBA – non-linear Boussinesq approximation
 THS – temperature dependent heat source parameter
 ESHS – exponential space-related heat source parameter
 MHD – magnetohydrodynamics

rate than Cu with H₂O as a base fluid.

The annular cylindrical region geometry for heat transfer is very essential in industrial applications such as turbomachines, engineering, heating, chemical industries, solar collectors and heat exchangers. Shahzadi and Nadeem [6] investigated the heat transfer in an inclined annular duct filled with nanofluids and observed that silver nanoparticles can enhance more pressure gradients than pure blood. Mixed convective flow in a vertical, concentric cylinder exposed to the heat source, thermal radiation in the presence of porous matrix was observed by Oni [7]. Mebarek-Oudina et al. [8] investigated the heat source aspect ratio increment in the fluid temperature over an annular-spaced vertical cylinder. Mebarek-Oudina et al. [9] has investigated natural oscillatory convective flow in a circular inclined annulus area filled with molten metal, obtaining the best stabilization for the system tilted at a 30° angle.

The linear Boussinesq approximation (LBA) truncates the density variation expansion of the Taylor series with temperature after the second term, assuming a linear density variation with temperature, and this LBA holds good only when the temperature difference is slightly varied. The mathematical model created using LBA becomes erroneous in other circumstances. The nonlinear Boussinesq approximation (NBA) with temperature as a result $\Delta\rho = -\rho\beta(T - T_w)^2$ was identified by Goren [10] in 1996. In the investigation of free convection in the presence of buoyancy force between two plates, by considering the non-

linear quadratic fluctuations in density with temperature, an increase in heat transfer is noticed by Vajravelu and Sastri [11]. The term $\Delta\rho/\rho$ is a nonlinear Boussinesq approximation using the Taylor series expansion. The mixed convective flow over vertical wavy-shaped surface in the presence of porous medium with nanofluid, using nonlinear Boussinesq approximation was inspected by Kameshwaran et al. [12].

The magnetohydrodynamics (MHD) is interaction of electrically conducting fluids in the influence of magnetic field, plays a major role in industrial applications of heat transfer analysis such as aircraft, designs of the fins, cooling of reactors, in geophysics and astrophysicists. Numerous studies have been conducted on MHD flow over the years. Sravan Kumar [13] investigated hybrid nanofluids as copper-ferrous oxide nanoparticles with ethylene glycol as base fluid and noticed that the heat flow rate of copper-ferrous oxide is reduced compared to copper with ethylene glycol as base fluid. Aladdin et al. [14] analysed the rate of heat transfer which is diminished in copper-aluminium oxide as compared to copper with water base fluids in MHD free convection flow over a plate. The experimental observation of forced convection over concentric tubes of heat exchangers of Cu-Al₂O₃ nanoparticles as high thermal conductivity is analysed by Phanindra et al. [15]. Sheikholeslami et al. [16] examined the transient natural convection flow along a moving vertical plate in nanofluids with isothermal and isoflux boundary conditions. Sheikholeslami and Ganji [17] studied the heat and mass trans-

fer in the influence of thermal radiation between two parallel plates of unsteady flow and discovered that an increment in radiation effect increases the boundary layer thickness of concentration. Suresh et al. [18] studied that heat transfer of copper-aluminium oxide/H₂O hybrid nanofluid with variation of pressure over a uniformly heated circular tube is increased when compared with pure water.

The study of viscous dissipation effects in the unsteady nanofluid flow over an exponentially moving vertical plate with Lorentz force, analysed by Sravan Kumar et al. [19], resulted in the enhancement of fluid velocity in the boundary layer. The comparative study of the dissipative and radiative flow of hybrid nanofluid between two coaxial cylinders studied by Hayat et al. [20] focuses on the viscous dissipation effects of hybrid nanofluids which are dominant when compared with nanofluids.

The novelty of the present work is nonlinear Boussinesq approximation which is $\Delta\rho/\rho = -[(T - T_0)\beta_0 + (T - T_0)^2\beta_1]$, an analysis including the MHD, radiation effects, and viscous dissipation effects of the hybrid nanofluid in a heated inclined porous concentric cylindrical region. The complicated non-dimensional set of nonlinear coupled equations is solved by a numerical method, using the 4th order RK method with a shooting technique to obtain solutions for the velocity and temperature. The outcomes are presented graphically and analysed in detail. The physical model focuses on industrial applications such as electronic cooling systems, environmental monitoring systems and medicine.

2. Mathematical formulation

The mixed convection of Cu-Al₂O₃-H₂O hybrid nanofluid of NBA approximation in an inclined two concentric cylinders is schematically depicted in Fig. 1.

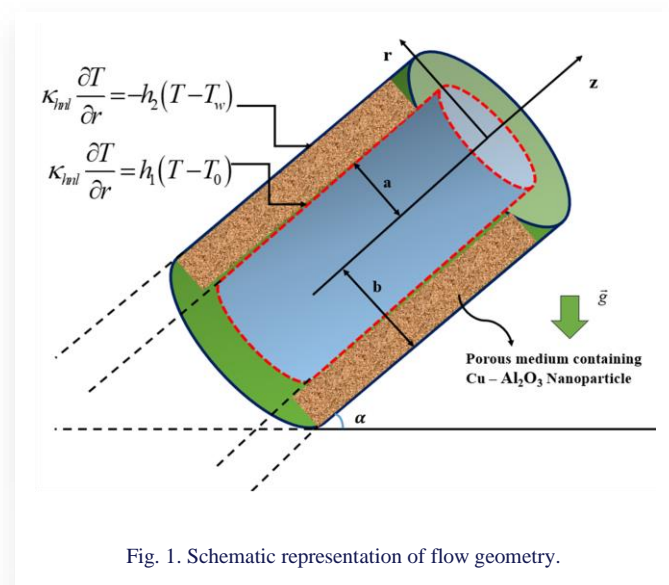


Fig. 1. Schematic representation of flow geometry.

The convective boundary conditions at the inner and outer cylinder respectively are $\kappa_{hmf} \frac{\partial T}{\partial r} = h_1(T - T_0)$ and $\kappa_{hmf} \frac{\partial T}{\partial r} = -h_2(T - T_w)$. The cylindrical coordinate system with the r -axis in the radial direction and the z -axis as the common axis is con-

sidered. The inner cylinder radius is $a \leq r \leq b$. The annulus with an unlimited length, and the fluid flow that is independent of z , is represented in the model given below (see Shahzadi and Nadeem [6], Oni [7]):

- Conservation of mass

$$\frac{1}{r} \left(\frac{\partial}{\partial r} (ru) \right) = 0, \quad (1)$$

- Conservation of momentum

$$\frac{\mu_{hmf}}{\rho_{hmf}} \frac{1}{2} \frac{\partial}{\partial r} \left(r \frac{\partial u}{\partial r} \right) - \frac{u\mu_{hmf}}{K\rho_{hmf}} - \frac{1}{\rho_{hmf}} \frac{\partial p}{\partial z} - \frac{1}{\rho_{hmf}} \sigma B_0^2 + \frac{g}{\rho_{hmf}} [(\rho\beta_0)_{hmf}(T - T_0) + (\rho\beta_1)_{hmf}(T - T_0)^2] \cos \alpha = 0, \quad (2)$$

- Conservation of energy

$$\begin{aligned} & \frac{\kappa_{hmf}}{(\rho C_p)_{hmf}} \left[\frac{1}{r} \frac{\partial}{\partial r} \left(r \frac{\partial T}{\partial r} \right) \right] + \frac{1}{(\rho C_p)_{hmf}} \frac{\partial q_r}{\partial r} + \\ & + \frac{Q_0}{(\rho C_p)_{hmf}} (T - T_0) + \frac{(T_w - T_0)}{(\rho C_p)_{hmf}} Q_e \exp\left(\frac{-nr}{a}\right) + \\ & + \left(\frac{\partial u}{\partial r} \right)^2 \frac{\mu_{hmf}}{(\rho C_p)_{hmf}} = 0, \end{aligned} \quad (3)$$

with the boundary conditions of dimensional form as given by Srinivasacharya et al. [21]:

$$\text{at } r = a: \quad u' = 0, \quad \kappa_{hmf} \frac{\partial T}{\partial r} = h_1(T - T_0), \quad (4)$$

$$\text{at } r = b: \quad u' = 0, \quad \kappa_{hmf} \frac{\partial T}{\partial r} = -h_2(T - T_w).$$

The volume fraction, thermal expansion coefficients, density, specific heat, dynamic viscosity, and thermal conductivity of hybrid nanofluid are given by (see [3,4,22–24]):

$$\phi = \phi_{Cu} + \phi_{Al_2O_3}, \quad (5)$$

$$\begin{aligned} (\rho\beta_0)_{hmf} &= ((1 - \phi) + \phi_{Cu} \frac{(\rho\beta_0)_{Cu}}{(\rho\beta_0)_f} + \\ & \phi_{Al_2O_3} \frac{(\rho\beta_0)_{Al_2O_3}}{(\rho\beta_0)_f}) (\rho\beta_0)_f, \end{aligned} \quad (6)$$

$$\begin{aligned} (\rho\beta_1)_{hmf} &= ((1 - \phi) + \phi_{Cu} \frac{(\rho\beta_1)_{Cu}}{(\rho\beta_1)_f} + \\ & \phi_{Al_2O_3} \frac{(\rho\beta_1)_{Al_2O_3}}{(\rho\beta_1)_f}) (\rho\beta_1)_f, \end{aligned} \quad (7)$$

$$\rho_{hmf} = \left((1 - \phi) + \phi_{Cu} \frac{\rho_{Cu}}{\rho_f} + \phi_{Al_2O_3} \frac{\rho_{Al_2O_3}}{\rho_f} \right) \rho_f, \quad (8)$$

$$\begin{aligned} (\rho C_p)_{hmf} &= ((1 - \phi) + \phi_{Cu} \frac{(\rho C_p)_{Cu}}{(\rho C_p)_f} + \\ & + \phi_{Al_2O_3} \frac{(\rho C_p)_{Al_2O_3}}{(\rho C_p)_f}) (\rho C_p)_f, \end{aligned} \quad (9)$$

$$\mu_{hmf} = \frac{1}{(1 - \phi)^{2.5}} \mu_{nf}, \quad (10)$$





$$\frac{\kappa_{hmf}}{\kappa_f} = \frac{\left(\frac{(\phi\kappa)_{Cu}+(\phi\kappa)_{Al_2O_3}}{\phi}\right)+(m-1)\kappa_f+(m-1)((\phi\kappa)_{Cu}+(\phi\kappa)_{Al_2O_3})-(m-1)\kappa_f\phi}{\left(\frac{(\phi\kappa)_{Cu}+(\phi\kappa)_{Al_2O_3}}{\phi}\right)+(m-1)\kappa_f+((\phi\kappa)_{Cu}+(\phi\kappa)_{Al_2O_3})-\kappa_f\phi} \quad (11)$$

The non-dimensional quantities are given by (see [7]):

$$\left. \begin{aligned} U &= \frac{u}{u_0}, & P &= \frac{pa}{u_0v_l} \\ \theta &= \frac{T-T_0}{T_w-T_0}, & R &= \frac{r}{a}, & Z &= \frac{z}{a} \end{aligned} \right\} \quad (12)$$

The values of thermophysical properties of hybrid nanofluids are tabulated in Table 1.

Table 1. H₂O, Cu and Al₂O₃ hybrid nanofluids thermophysical properties at 300 K.

Properties	Cu	Al ₂ O ₃	H ₂ O	Different shape of nanoparticle	m
ρ, kg·m ⁻³	8933	3970	997.1		3
κ, W·m ⁻¹ ·K ⁻¹	401	40	0.613		5.7
β·10 ⁻⁵ , K ⁻¹	1.67	0.85	21		4.8
μ, kg·m ⁻¹ ·s ⁻¹	-	-	0.00089		3.7

Further, the dimensionless quantities describing thermophysical properties are denoted by:

$$\begin{aligned} A_1 &= \frac{1}{(1-\phi)^{2.5}}, \\ A_2 &= (1-\phi) + \phi_{Cu} \frac{(\rho\beta_0)_{Cu}}{(\rho\beta_0)_f} + \phi_{Al_2O_3} \frac{(\rho\beta_0)_{Al_2O_3}}{(\rho\beta_0)_f}, \\ A_3 &= (1-\phi) + \phi_{Cu} \frac{\rho_{Cu}}{\rho_f} + \phi_{Al_2O_3} \frac{\rho_{Al_2O_3}}{\rho_f}, \\ A_4 &= \frac{\left(\frac{(\phi\kappa)_{Cu}+(\phi\kappa)_{Al_2O_3}}{\phi}\right)+(m-1)\kappa_f+(m-1)((\phi\kappa)_{Cu}+(\phi\kappa)_{Al_2O_3})-(m-1)\kappa_f\phi}{\left(\frac{(\phi\kappa)_{Cu}+(\phi\kappa)_{Al_2O_3}}{\phi}\right)+(m-1)\kappa_f+((\phi\kappa)_{Cu}+(\phi\kappa)_{Al_2O_3})-\kappa_f\phi} \end{aligned}$$

Using non-dimensional quantities given by Eqs. (12) and thermophysical properties represented by Eqs. (5)–(11), Eqs. (1)–(4) are transformed to the following forms:

$$A_1 \left(\frac{d^2U}{dR^2} + \frac{1}{R} \frac{dU}{dR} \right) + Mc(A_2\theta + A_3Qc\theta^2) \cos(\alpha) - \frac{A_1}{Da} U - p - M^2U = 0, \quad (13)$$

$$\begin{aligned} \frac{A_4}{Pr} \left(\frac{d^2\theta}{dR^2} + \frac{1}{R} \frac{d\theta}{dR} \right) + Q_T\theta + Q_E \exp(-nR) + \\ - \frac{N}{Pr} \frac{d^2\theta}{dR^2} + A_1 Ec \left(\frac{dU}{dR} \right)^2 = 0, \end{aligned} \quad (14)$$

$$\text{at } R = 1: \quad U = 0, \quad \frac{d\theta}{dR} = \frac{Bi_1}{A_4} \theta, \quad (15)$$

$$\text{at } R = \lambda: \quad U = 0, \quad \frac{d\theta}{dR} = \frac{Bi_2}{A_4} (1 - \theta).$$

The physical quantities like non-dimensional Nusselt numbers (Nu₁ and Nu_λ) and skin friction coefficients (τ₁ and τ_λ) are defined as [25]:

$$\text{at } R = 1: \quad Nu_1 = \frac{\kappa_{hnl}}{\kappa_l} \left(\frac{d\theta}{dR} \right)_{R=1}, \quad \tau_1 = \frac{\mu_{hnl}}{\mu_l} \left(\frac{dU}{dR} \right)_{R=1} \quad (16)$$

$$\text{at } R = \lambda: \quad Nu_\lambda = \left(\frac{\kappa_{hnl}}{\kappa_l} + N \right) \left(\frac{d\theta}{dR} \right)_{R=\lambda}, \quad \tau_\lambda = \left(\frac{\mu_{hnl}}{\mu_l} + N \right) \left(\frac{dU}{dR} \right)_{R=\lambda}$$

3. Numerical method

The non-dimensional Eqs. (13)–(14) with the dimensionless boundary condition Eq. (15) are numerically solved using the 4th order RK shooting technique method [24]. By using [U, U', θ, θ'] = [y₁, y₂, y₃, y₄], the system of equations can be written in the first-order differential equations as follows:

$$\begin{aligned} y_1' &= y_2 \\ y_2' &= \frac{-1}{A_1} \left(Mc(A_2y_3 + A_3Qc y_3^2) \cos \alpha - \frac{A_1 y_1}{Da} - p - M^2 y_1 \right) - \frac{y_2}{R}, \quad (17) \\ y_3' &= y_4 \\ y_4' &= \frac{-Pr}{A_4} \left(Q_T y_3 + Q_E \exp(-nR) - \frac{N y_3}{Pr} + A_1 Ec y_1^2 \right) - \frac{y_4}{R} \end{aligned}$$

with boundary conditions:

$$\text{at } R = 1: \quad y_1 = 0, \quad y_4 = \frac{Bi_1}{A_4} y_3, \quad (18)$$

$$\text{at } R = \lambda: \quad y_1 = 0, \quad y_4 = \frac{Bi_2}{A_4} (1 - y_3).$$

and corresponding initial conditions:

$$\begin{aligned} y_1(1) &= 0, \quad y_2(1) = t_1, \\ y_3(1) &= t_2, \quad y_4(1) = \frac{Bi_1}{A_4} t_2, \end{aligned} \quad (19)$$

where t₁ and t₂ are the initial values. The initial conditions are approximated to satisfy the boundary conditions. Table 2 gives the information of Q_T for Nusselt number at r=1.

4. Results and discussion

The analysis of heat transfer between two concentric cylinders in an annulus is presented through graphs and tables. Figures 2–15 show various effects such as those of MHD (M), radiation (N), viscous dissipation (Ec), volume fraction (φ), etc. on velocity U(R) and temperature θ(R). The data on graphs and in tables are obtained for the fixed effective parameters, such as Mc = 2, Qc = 0.5, α = π/4, Da = 0.1, Q_T = 0.01, Q_E = 0.1, Pr = 6.0674, Bi₁ = Bi₂ = 0.3, M = 0.5, Ec = 0.1, N = 1 and φ = 0.01 [25].

In the performance of magnetic field, Fig. 2 displays the velocity profiles for different magnetic parameter (M²) values. As M² increases, the fluid velocity decreases. This is due to the Lorentz force, a resistive force generated by the interaction of the transverse magnetic field with in the convective fluid. This force opposes the flow, reducing the fluid velocity and leading to a thin momentum boundary layer. MHD is used in medicinal field to study plasma of human body in biological and environmental monitoring systems. The effect of viscous dissipation in

temperature graph observed in Fig. 3 shows that the thickness of thermal boundary increases with increasing Ec , which is due to the conversion of mechanical energy into thermal energy. This results in additional heating of the fluid, leading to a rise in temperature within the boundary layer and an enhancement of heat transfer.

In Figs. 4–5, we observe that the radiation effect (N) decreases the velocity for different values of N due to the temperature difference and boundary layer thickness. In the temperature plot, as temperature increases for different values of N due to its increased thermal conductivity, addition of nanoparticles may lead to influencing radiative heat transfer between the cylinders. Hybrid nanofluids can be used as a coolant in electronic devices such as computers, televisions and smartphones, so as to prevent overheating and improve dissipation of heat.

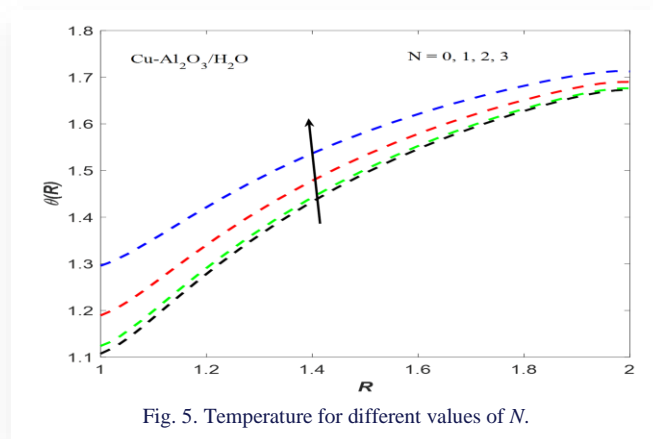


Fig. 5. Temperature for different values of N .

The concentration of nanoparticles refers to volume fraction (ϕ) and from Figs. 6 and 7 we noticed that the volume fraction in velocity profile decreases, as nanoparticle concentration increases. Due to the suspension of nanoparticles in the base fluids, density is increased, leading to a decrement in velocity profiles of the fluid in a porous cylinder. Whereas, in the temperature profile, the energy increases as the volume fraction increases. This is due to the good thermal conductivity of the nanofluid and larger surface area of nanoparticles, which enable more efficient heat transfer.

In Figs. 8 and 9, we observe the combined effect of exponentially related heat source parameter (ESHS) (Q_E) on $U(R)$ and $\theta(R)$, showing an increment in Q_E leading to more effective heat transfer in increased velocity. The temperature profile for varied Q_E is increased, because the ESHS mechanism gives an additional heat source to the system. It can be seen that the velocity increases for platelet-shaped nanoparticles when compared to cylinder, brick, and spherical-shaped nanoparticles, as shown in Fig. 10. The temperature profiles fluctuate, as seen in Fig. 11, with the platelet-shaped nanoparticles having a high temperature at the inner cylinder and a lower profile at the outer cylinder when compared to the cylinder, brick, and spherical-shaped nanoparticles.

In Fig. 12, we observe that as quadratic convection Q_c increases, the momentum profile also increases because of its strong buoyancy force. Further, a higher momentum is observed in the quadratic convection than in LBA. The behaviour of the velocity graphs for the various values is plotted in Fig. 13, and it is observed that permeability for the lower value of Da gives an increment in the momentum of the porous region compared to the clear region $Da = 0$. From Fig. 14 we can visualize the effect of mixed convection (Mc) on the velocity, which increases with Mc due to the domination of buoyancy force to the inertial force. This results in an effective improvement of heat transfer. As the angle of inclination α increases, the velocity decreases due to the least domination of acceleration by gravity, as shown in Fig. 15.

By comparing results of Thriveni and Mahantesh [25] (see Table 2) we noticed that the present study outcomes are in good agreement as regards Q_T values of the Nusselt number at the lower wall. Table 3 illustrates the significance of skin friction for different effects such as M^2 , Mc , Q_c , and Da , showing an increasing trend of the velocity at the surface. Though the angle

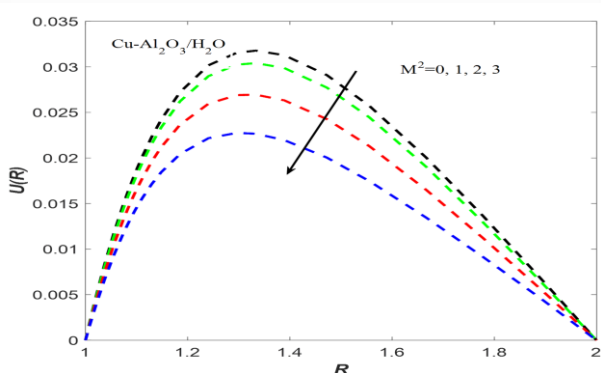


Fig. 2. Velocity for different values of M^2 .

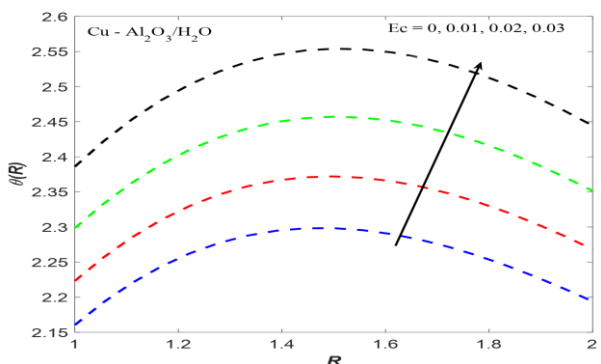


Fig. 3. Temperature for different values of Ec .

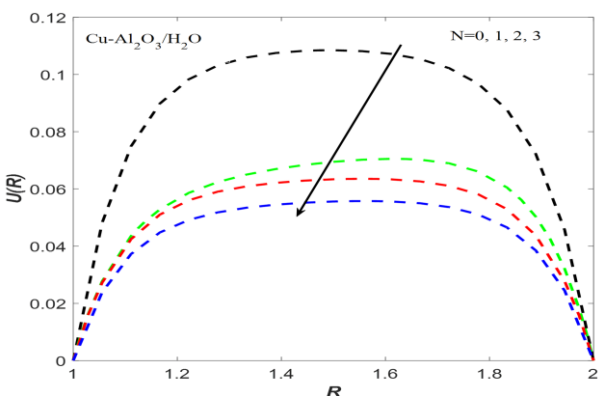


Fig. 4. Velocity for different values of N .

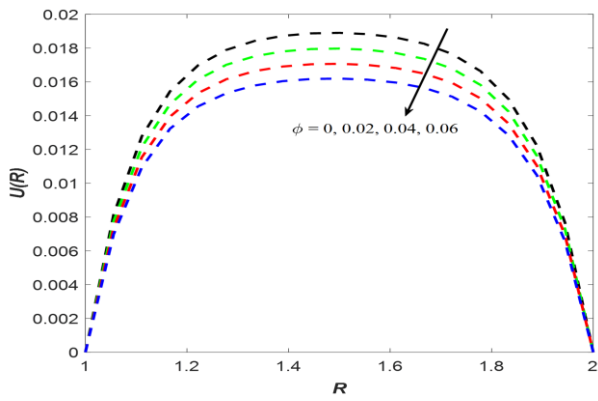


Fig. 6. Velocity for different values of ϕ .

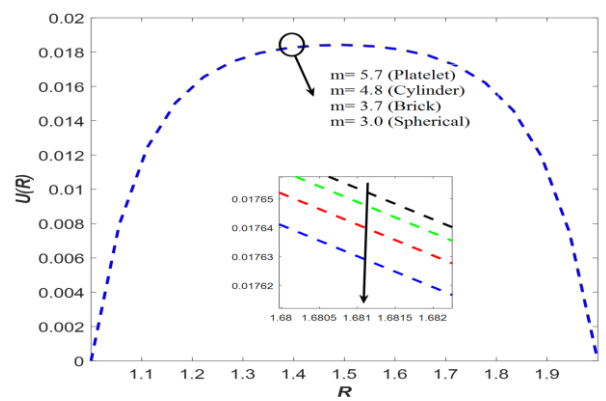


Fig. 10. Velocity for different values of m .

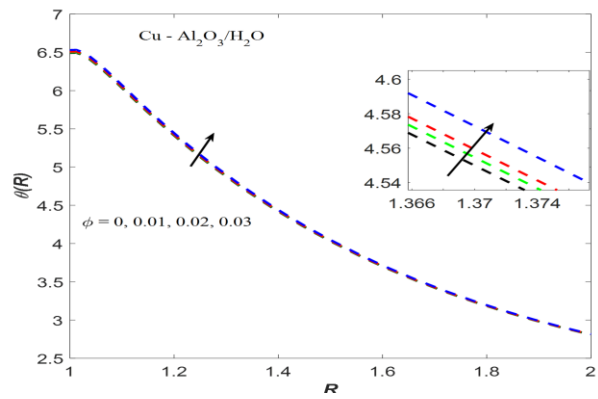


Fig. 7. Temperature for different values of ϕ .

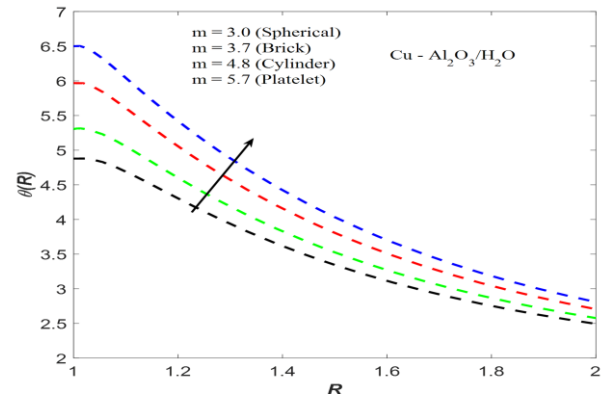


Fig. 11. Temperature for different values of m .

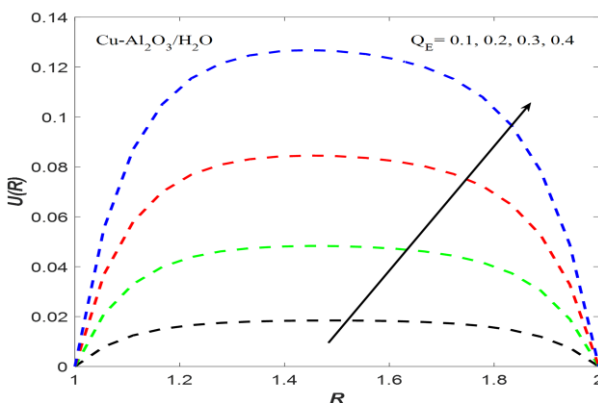


Fig. 8. Velocity for different values of Q_E .

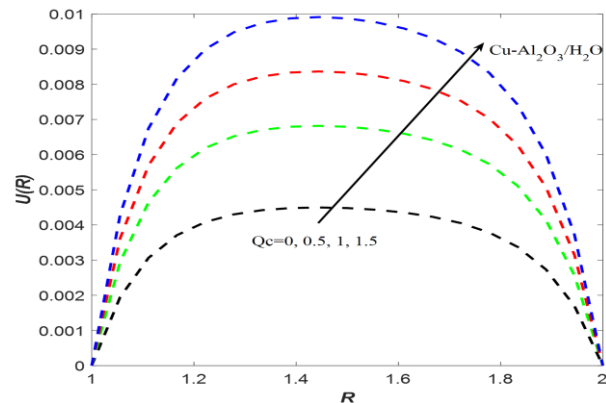


Fig. 12. Velocity for different values of Q_c .

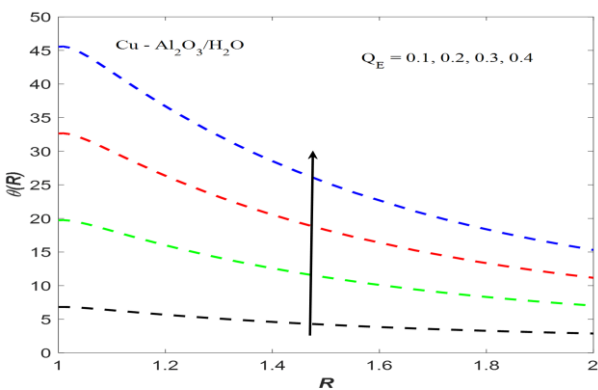


Fig. 9. Temperature for different values of Q_E .

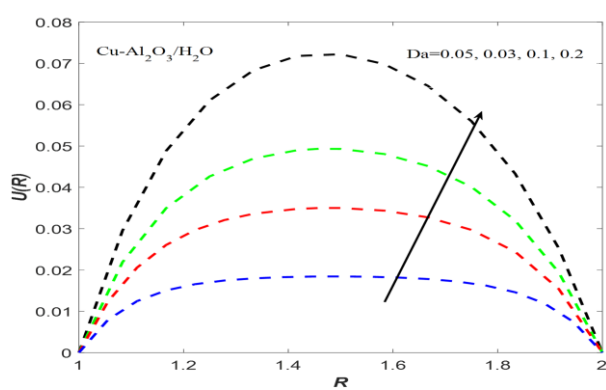


Fig. 13. Velocity for different values of Da .

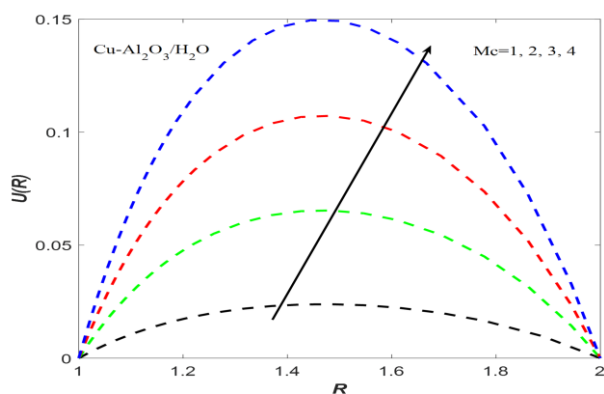
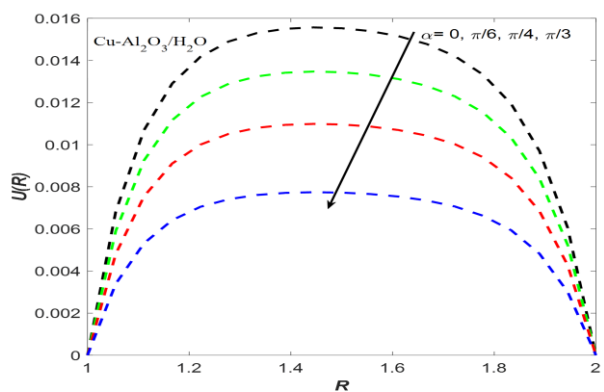

 Fig. 14. Velocity for different values of Mc .

 Fig. 15. Velocity for different values of α .

 Table 2. The Nusselt number for different values of Q_T at $r=1$.

Q_T	Thiriveni and Mahanthesh [25]	Present work
0.5	1.571404	1.571405
1.0	1.716981	1.716982
1.5	1.882604	1.882605
2.0	2.072277	2.072278
2.5	2.291116	2.291117
3.0	2.545765	2.545766

 Table 3. Numerical values of τ_1 and τ_2 for various values of M^2 , Mc , Q_c , Da and α when $Pr = 6.0674$, $Q_T = 0.01$, $Q_E = 0.1$, $Bi_1 = Bi_2 = 0.03$ and $\phi = 2\%$.

M^2	Mc	Q_c	Da	α	τ_1	τ_2
1	2	0.5	0.1	$\pi/4$	0.451468	0.484422
2					0.562719	0.594243
3					0.662388	0.683438
	2				0.481467	0.434245
	2.5				0.601915	0.542874
	3				0.722363	0.651503
		0.1			0.374082	0.333169
		0.2			0.400928	0.358438
		0.3			0.427774	0.383707
			0.05		0.351276	0.332389
			0.07		0.412666	0.381011
			0.09		0.460956	0.418489
				$\pi/6$	0.589747	0.531900
				$\pi/4$	0.481467	0.434245
				$\pi/3$	0.340353	0.306978

gets smaller, there is an increase in velocity at the lower wall of the cylinder.

5. Conclusions

The hybrid nanofluid flow in a convectively heated system of two concentric cylinders containing porous medium with the effects of MHD, thermal radiation, viscous dissipation, as well as exponential space-related heat source parameter and temperature-dependent heat source parameter was considered. The non-linear and coupled equations were numerically solved using the shooting 4th order RK method. The analysis of MHD, thermal radiation, viscous dissipation, volume fraction, and Darcy number are discussed graphically. The findings of this study are as follows:

1. The strong magnetic effect (M^2) enhances effective heat transfer by the influence of Lorentz forces, which results in reduction of the boundary layer thickness.
2. The effect of viscous dissipation (Ec) on the temperature profiles is strong due to conversion of mechanical energy into thermal energy, and leads to an overall increase in heat transfer.
3. The thermal radiation effect (N) increases the heat flow rate, and enhances the potential of overall thermal performance.
4. The rate of heat transfer of hybrid nanofluids is higher when compared to pure nanofluids.

References

- [1] Choi, S.U.S., & Eastman, J. (1995). Enhancing thermal conductivity of fluids with nanoparticles. *Developments and Applications of Non-Newtonian Flows*, 66, 99–105.
- [2] Suresh, S., Venkataraj, K.P., Selvakumar, P., & Chandrasekar, M. (2012). Effect of Al_2O_3 -Cu/water hybrid nanofluid in heat transfer. *Experimental Thermal and Fluid Science*, 38, 54–60. doi: 10.1016/j.expthermflusci.2011.11.007
- [3] Devi, S.S.U., & Devi, S.P.A. (2016). Numerical investigation of three-dimensional hybrid $Cu-Al_2O_3$ /water nanofluid flow over a stretching sheet with effecting Lorentz force subject to Newtonian heating. *Canadian Journal of Physics*, 94(5), 490–496. doi: 10.1139/cjcp-2015-0799
- [4] Kanchana, C., Siddheshwar, P.G.S., & Zhao, Y. (2019). A study of Rayleigh-Bénard convection in hybrid nanoliquids with physically realistic boundaries. *The European Physical Journal Special Topics*, 228(12), 2511–2530. doi: 10.1140/epjst/e2019-900074-1
- [5] Waini, I., Ishak, A., Grosan, T., & Pop, I. (2020). Mixed convection of a hybrid nanofluid flow along a vertical surface embedded in a porous medium. *International Communications in Heat and Mass Transfer*, 114, 104565. doi: 10.1016/j.icheatmasstransfer.2020.104565
- [6] Shahzadi, I., & Nadeem, S. (2017). Inclined magnetic field analysis for metallic nanoparticles submerged in blood with convective boundary condition. *Journal of Molecular Liquids*, 230, 61–73. doi: 10.1016/j.molliq.2017.01.008
- [7] Oni, M.O. (2017). Combined effect of heat source, porosity and thermal radiation on mixed convection flow in a vertical annulus: An exact solution. *Engineering Science and Technology, an International Journal*, 20(2), 518–527. doi: 10.1016/j.jestch.2016.12.009

- [8] Mebarek-Oudina, F., Aissa, A., Mahanthesh, B., & Öztöp, H.F. (2020). Heat transport of magnetized Newtonian nanoliquids in an annular space between porous vertical cylinders with discrete heat source. *International Communications in Heat and Mass Transfer*, 117, 104737. doi: 10.1016/j.icheatmasstransfer.2020.104737
- [9] Mebarek-Oudina, F., Bessaih, R., Mahanthesh, B., Chamkha, A.J., & Raza, J. (2020). Magneto-thermal-convection stability in an inclined cylindrical annulus filled with a molten metal. *International Journal of Numerical Methods for Heat & Fluid Flow*, 31(4), 1172–1189. doi: 10.1108/hff-05-2020-0321
- [10] Goren, S.L. (1996). On free convection in water at 4°C. *Chemical Engineering Science*, 21(6–7), 515–518. doi: 10.1016/0009-2509(66)85065-0
- [11] Vajravelu, K., & Sastri, K.S. (1977). Fully developed laminar free convection flow between two parallel vertical walls. *International Journal of Heat and Mass Transfer*, 20(6), 655–660. doi: 10.1016/0017-9310(77)90052-7
- [12] Kameswaran, P.K., Vasu, B., Murthy, P.V.S.N., & Gorla, R.S.R. (2016). Mixed convection from a wavy surface embedded in a thermally stratified nanofluid saturated porous medium with non-linear Boussinesq approximation. *International Communications in Heat and Mass Transfer*, 77, 78–86. doi: 10.1016/j.icheatmasstransfer.2016.07.006
- [13] Kumar, T.S. (2021). Hybrid nanofluid slip flow and heat transfer over a stretching surface. *Partial Differential Equations in Applied Mathematics*, 4, 100070. doi: 10.1016/j.padiff.2021.100070
- [14] Aladdin, N.A.L., Bachok, N., & Pop, I. (2020). Cu-Al₂O₃/water hybrid nanofluid flow over a permeable moving surface in presence of hydromagnetic and suction effects. *Alexandria Engineering Journal*, 59(2), 657–666. doi: 10.1016/j.aej.2020.01.028
- [15] Phanindra, Y., Kumar, S.D., & Pugazhendhi, S. (2018). Experimental Investigation on Al₂O₃ & Cu/Oil Hybrid Nanofluid using Concentric Tube Heat Exchanger. *Materials Today: Proceedings*, 5(5), 12142–12150. doi: 10.1016/j.matpr.2018.02.192
- [16] Sheikholeslami, M., Bandpy, M.G., Ellahi, R., & Zeeshan, A. (2014). Simulation of MHD CuO–water nanofluid flow and convective heat transfer considering Lorentz forces. *Journal of Magnetism and Magnetic Materials*, 369, 69–80. doi: 10.1016/j.jmmm.2014.06.017
- [17] Sheikholeslami, M., & Ganji, D.D. (2014). Unsteady nanofluid flow and heat transfer in presence of magnetic field considering thermal radiation. *Journal of the Brazilian Society of Mechanical Sciences and Engineering*, 37(3), 895–902. doi: 10.1007/s40430-014-0228-x
- [18] Suresh, S., Venkitaraj, K.P., Hameed, M.S., & Sarangan, J. (2014). Turbulent Heat Transfer and Pressure Drop Characteristics of Dilute Water Based Al₂O₃–Cu Hybrid Nanofluids. *Journal of Nanoscience and Nanotechnology*, 14(3), 2563–2572. doi: 10.1166/jnn.2014.8467
- [19] Sravan Kumar, T., Dinesh, P.A., & Makinde, O.D. (2020). Impact of Lorentz Force and Viscous Dissipation on Unsteady Nanofluid Convection Flow over an Exponentially Moving Vertical Plate. *Mathematical Models and Computer Simulations*, 12(4), 631–646. doi:10.1134/s2070048220040110
- [20] Hayat, T., Yazman, M., Muhammad, K., & Momani, S. (2023). Radiative and dissipative flow of hybrid nanofluid between two coaxial cylinders: A comparative numerical study. *Alexandria Engineering Journal*, 71, 79–88. doi: 10.1016/j.aej.2023.03.030
- [21] Srinivasacharya D., & Hima Bindu, K. (2018). Entropy generation due to micropolar fluid flow between concentric cylinders with slip and convective boundary conditions. *Ain Shams Engineering Journal*, 9(2), 245–255. doi: 10.1016/j.asej.2015.10.016
- [22] Thriveni K., & Mahanthesh, B. (2020). Nonlinear Boussinesq buoyancy driven flow and radiative heat transport of magnetohybrid nanoliquid in an annulus: A statistical framework. *Heat Transfer*, 49(8), 4759–4782. doi: 10.1002/htj.21851
- [23] Lakshmi, K.M., Siddheshwar, P.G., & Laroze, D. (2020). Natural convection of water-copper nanoliquids confined in low-porosity cylindrical annuli. *Chinese Journal of Physics*, 68, 121–136. doi: 10.1016/j.cjph.2020.09.008
- [24] Kierzenka, J., & Shampine, L.F. (2001). A BVP solver based on residual control and the Maltab PSE. *ACM Transactions on Mathematical Software*, 27(3), 299–316. doi: 10.1145/502800.502801
- [25] Thriveni, K., & Mahanthesh, B. (2021). Sensitivity computation of nonlinear convective heat transfer in hybrid nanomaterial between two concentric cylinders with irregular heat sources. *International Communications in Heat and Mass Transfer*, 129, 105677. doi: 10.1016/j.icheatmasstransfer.2021.105677